Received: 31 August 2021 | Revised: 13 December 2021 | Accepted: 15 December 2021

DOI: 10.1111/ppl.13615

SPECIAL ISSUE ARTICLE

Physiologia Plantarum

Acclimation to elevated CO_2 affects the C/N balance by reducing de novo N-assimilation

Konrad Krämer | Gabi Kepp | Judith Brock | Simon Stutz | Arnd G. Heyer

Institute of Biomaterials and Biomolecular Systems, Department of Plant Biotechnology, University of Stuttgart, Stuttgart, Germany

Correspondence
Arnd G. Heyer, Institute of Biomaterials and Biomolecular Systems, Department of Plant Biotechnology, University of Stuttgart, Pfaffenwaldring 57, 70569 Stuttgart, Germany.
Email: arnd.heyer@bio.uni-stuttgart.de

Funding information
Landesgraduiertenförderung Baden-Württemberg

Edited by Y. Gibon

Abstract

Plants exposed to elevated atmospheric CO_2 concentrations show an increased photosynthetic activity. However, after prolonged exposure, the activity declines. This acclimation to elevated CO_2 is accompanied by a rise in the carbon-to-nitrogen ratio of the biomass. Hence, increased sugar accumulation and sequential downregulation of photosynthetic genes, as well as nitrogen depletion and reduced protein content, have been hypothesized as the cause of low photosynthetic performance. However, the reason for reduced nitrogen content in plants at high CO_2 is unclear. Here, we show that reduced photorespiration at increased CO_2-to-O_2 ratio leads to reduced *de novo* assimilation of nitrate, thus shifting the C/N balance. Metabolic modeling of acclimated and non-acclimated plants revealed the photorespiratory pathway to function as a sink for already assimilated nitrogen during the light period, providing carbon skeletons for *de novo* assimilation. At high CO_2, low photorespiratory activity resulted in diminished nitrogen assimilation and eventually resulted in reduced carbon assimilation. For the *hpr1-1* mutant, defective in reduction of hydroxy-pyruvate, metabolic simulations show that turnover of photorespiratory metabolites is expanded into the night. Comparison of simulations for *hpr1-1* with those for the wild type allowed investigating the effect of a perturbed photorespiration on N-assimilation.

1 | INTRODUCTION

Rising emissions have led to a dramatic increase of atmospheric CO_2 concentration during the last decade (IPCC, 2014; Solomon et al., 2009), and despite intensive research, for example, on consequences for productivity at the ecosystem level (Liu et al., 2018; Long et al., 2004), many questions regarding the effects of elevated CO_2 (eCO_2) on plant metabolism are still unanswered (Misra & Chen, 2015). Plants benefit from eCO_2 concentrations by an increased net photosynthesis (NPS) rate. However, after a period of several days to weeks of growth in eCO_2 a decline is observed, which is called acclimation to eCO_2 (Griffin & Seemann, 1996; Smith & Dukes, 2013). A multitude of studies have shown that various plant species show this response, including important crops (Gutiérrez et al., 2013; Shimono et al., 2010), and even though many theories have been put forward, the physiological basis for acclimation to eCO_2 is still unclear.

One possible explanation is down regulation of photosynthesis (PS) due to an accumulation of carbohydrates (Dabu et al., 2019; Gámez et al., 2020; Kizildeniz et al., 2021). A clear increase of glucose, fructose, and starch was observed in *Arabidopsis thaliana* when grown for longer periods at eCO_2 (Cheng et al., 1998). High carbohydrate levels correspond to a dilution of nitrogen (N) containing compounds such as amino acids (AA) and protein, and the resulting low level of ribulose-1,5-bisphosphate-carboxylase/-oxygenase (RUBISCO) (Chen et al., 2005; Cheng et al., 1998; Paul &

Driscoll, 1997) could also explain reduced PS per weight unit as proposed by Gifford et al. (2000), Kuehny et al. (1991), and Wong (1990). Other concepts explaining acclimation to eCO_2 are directly related to N acquisition. Decreased stomatal conductance resulting from higher internal CO_2 concentrations in leaves may cause low transpiration rates, thus interfering with mineral uptake and transport (Ainsworth & Rogers, 2007; Shi et al., 2021). Nitrogen partitioning within the plant and its availability to photosynthetically active leaves was shown to contribute to acclimation in soybean (Kanemoto et al., 2009), and its allocation to either biomass or optimization of the photosynthetic apparatus is important for crop yield (Biernath et al., 2013).

Because assimilation of N in the form of AA requires carbon skeletons, the provision of α-ketoglutarate (α-KG) takes a central role, thus tightly linking the mitochondrial citrate cycle to *de novo* N fixation. Considering that glycolysis and day respiratory CO_2 release are, at least to some extent, inhibited by light, Gauthier et al. (2010) questioned the origin of α-KG from recently assimilated carbon and reported that remobilization of existing carbon pools is important for α-KG provision. However, an alternative route to C-skeletons for AA synthesis via malate produced in the chloroplast in the so-called pyruvate branch of the photorespiratory pathway has been proposed (Bloom et al., 2020).

A striking feature of eCO_2 is a reduction of the oxygenase activity of RUBISCO, which is the entry point into photorespiratory metabolism (Keys, 2006). This metabolic route links carbon (C) and N metabolism, most obviously by producing the AA glycine (Gly), but has an impact on various other metabolic pathways, including sulfur assimilation and secondary metabolism (Abadie et al., 2021; Timm et al., 2021). Recently, it was shown that in C3, but not in C4, plants eCO_2 improved the use of ammonium as a nitrogen source (Wang et al., 2020). However, interactions between nitrogen metabolism, PS and photorespiration (PR) are not yet well understood. Liang et al. (2021) proposed that in rice, which is generally believed to oversize its photosystem antenna, PR has a function of stabilizing the C/N balance by consuming photosynthetic products and providing AAs for nitrogen metabolism, thus preventing a continuous increase in the C/N ratio, which would induce premature senescence and yield reduction.

To investigate whether PR functions as a gatekeeper between carbon and nitrogen assimilation, we set up a mathematical model that allows simulation of fluxes through PR and PS, as well as calculation of *de novo* N fixation. We used this model to simulate fluxes in plants exposed to either short-term or prolonged exposure to eCO_2. Under the latter conditions, photosynthetic acclimation caused a marked reduction in NPS. This was more pronounced in the *hpr1-1* mutant of *A. thaliana*, which is defective in the peroxisomal hydroxypyruvate-reductase (HPR). This enzyme catalyzes the last step in the PR pathway providing glycerate for re-import into the chloroplast (Timm et al., 2008). Instead, the mutant accumulates high levels of serine (Ser) and Gly, thus altering the balance between C and N metabolism.

2 | MATERIALS AND METHODS

2.1 | Plant materials and growth conditions

Arabidopsis thaliana wild-type Col-0 and the mutant *hpr1-1* (SALK067724) were grown in soil (seedling substrate, Klasmann-Deilmann GmbH) in a growth chamber with 8/16 h light/dark regime (100 μmol m^{-2} s^{-1}; 22/16°C). The *hpr1-1* mutant was obtained from the group of Hermann Bauwe at the University of Rostock; for details, see Timm et al. (2008). All plants were grown at ambient CO_2 concentrations (450 ± 20 ppm) for the first week. Afterward, half of them were transferred to eCO_2 (1000 ± 20 ppm), whereas the other plants were transferred after 44 days. Plants were harvested after 46 days of cultivation. Plants that grew longer at eCO_2 concentrations are denominated acclimated, while those that spent only 48 h at eCO_2 are termed non-acclimated. To exclude the possibility that the plants differ in developmental states, leaves were counted of 10 plants per condition. A Fisher's exact test resulted in a *p*-value of 0.9889. Thus, there was no difference in the developmental stage of the plants. From both sets of plants, samples were taken every 2 h over a full diurnal cycle, with the time point at the end of the night harvested only once. This time point was used as the start and end of the simulations.

To examine metabolic changes caused by shifting plants from ambient CO_2 concentrations to eCO_2, Col-0, and the *hpr1-1* mutant were grown at ambient CO_2 levels and harvested at the beginning and end of light phase.

2.2 | Gas-exchange measurements and calculation of PR

The CO_2 uptake by the plants was measured as already described by Nägele et al. (2010). An entire rosette was measured over 24 h in a growth chamber with 8/16 h light/dark regime (100 μmol m^{-2} s^{-1}; 22/16°C, 65% RH, 1000 ppm CO_2). Dark respiration was calculated as a mean over the entire dark phase. While NPS was measured as CO_2 exchange of whole plant rosettes with the atmosphere, the input into PR was calculated according to Sharkey (1988) (Equations (1) and (2)). For the CO_2 concentration at the carboxylation site, 600 ppm were used.

$$v_0 = (A + R_d)/(\phi^{-1} - 0.5) \quad (1)$$

where v_0 is the oxygenation rate, A is the photosynthetic rate, R_d is the respiration during the night, and ϕ is the ratio between oxygenation and carboxylation of RUBISCO. R_d is the mean value of the entire night without the first 5 min of the dark phase.

$$\Phi = (2\tau*)/[CO_2] \quad (2)$$

where ϕ is the ratio between oxygenation and carboxylation, τ^* is the CO_2 compensation point in the absence of dark respiration and [CO_2]

is the CO_2 concentration at the carboxylation site. τ^* was measured according to the method described by Brooks and Farquhar (1985).

2.3 | Metabolic profiling

Gas-chromatography coupled to mass spectrometry (GC–MS)/MS analysis samples were extracted using 750 µl methanol with 25 nmol ribitol as internal standard. After adding methanol, samples were incubated for 15 min at 70°C and agitated for 10 min at RT followed by centrifugation (5 min 17,000*g*). The supernatant was transferred to a new vessel. Next, 400 µl H_2O was added to the pellet, incubated at 95°C for 10 min followed by shaking for 10 min at RT. Then, samples were centrifuged (5 min 17,000*g*) and the supernatant pooled with solution from the previous step. Afterward, 300 µl H_2O and 200 µl chloroform were added to the suspension. After centrifugation (2 min 17,000g), the two phases were separated. Only the polar phase was used for analysis and dried in a speedvac. The dried samples were derivatized using 20 µl of methoxamine dissolved in pyridine (40 mg ml^{-1}) by incubation for 90 min at 30°C. Afterward, 80 µl *N*-methyl-*N*-(trimethylsilyl)trifluoroacetamide were added and the mixture incubated for 30 min at 50°C. The metabolites were measured using GC–MS/MS. For injection, 1 µl of the derivatized sample was used. The GC–MS/MS device was a GCMS-TQ8040 (Shimadzu). Helium was used as carrier gas with a column flow of 1.12 ml min^{-1}, and for the stationary phase, a 30 m Optima 5MS-0.25 µm fused silica capillary column was used. The injection temperature was 230°C. The transfer line and ion source were set to 250 and 200°C, respectively. The initial temperature of the column oven was 80°C and this was increased by 15°C per min until the final temperature of 330°C was reached, which was held for 6 min. After a solvent delay of 4.6 min, spectra of the MS device were recorded in the multiple reaction mode with specific target-ions for each metabolite. External standards were used for quantification. Besides metabolic profiling via GC–MS/MS analysis, additional metabolites, i.e. starch, hexose phosphates (HP), carboxylic acids (fumaric acid, malic acid, and citric acid) as well as minerals (nitrate, phosphate, and sulfate) and the total AA pool, were quantified by HPLC as described previously (Küstner et al., 2019). Levels of malate and fumarate (MF) were summed up as MF pool. For the carboxylic acids and minerals, quantification was performed at the beginning, the middle and the end of the light phase—as well as the middle of the night. The HP were measured at every second time point. Data for the remaining time points were obtained by spline interpolation.

2.4 | Enzyme activities

The HPR activity was determined according to Bauwe (2017). The activities of the enzymes sucrose-phosphate-synthase (SPS), glucokinase, and fructokinase were measured according to Küstner et al. (2019). All enzyme activities were determined at the beginning, middle and end of the light phase, as well as in the middle of the night. Values for the remaining time points were calculated by spline interpolation.

2.5 | Simulations

For simulations, the Github-version of the R-package "paropt" was used (Krämer et al., 2020) and https://github.com/Konrad1991/paropt). During each simulation, the system of ordinary-differential-equations (ODE) is repeatedly solved with different parameter sets. Hence, for each parameter set, a unique state solutions is produced. This *in silico* solution is compared to the measured states to yield an error which is used to evaluate the parameters. Based on the errors of each set, the optimizer updates the parameter sets. For optimization, the particle swarm optimization algorithm was used; for details of implementation, see (Akman et al., 2018; Krämer et al., 2020; Sengupta et al., 2018). The package uses the SUNDIALS Software to solve the ODE-system (Hindmarsh et al., 2005). Because of its superiority in solving stiff ODE-systems, the backward-differential-equation solver was used (Hindmarsh et al., 2005) with relative tolerance set to 1e-6 and absolute tolerances set for each state to 1e-8. For each run, a different seed was set for random number generation. The code of the ODE-system can be found in the supplement.

The *on/off* mode of illumination in the plant growth chamber caused abrupt transitions between day and night leading to overshooting of changes in reaction rates (Küstner et al., 2019). To allow calculation of a smooth day-night-transition, an interval from 0.1 h before and 0.1 h after start of the dark period was defined. Within this interval, supporting data points for the ODE-solver were generated for PS and PR. To achieve this, the property of the tangens hyperbolicus to show increasing values of a sigmoid form from 0 to 1 for the interval [0,2] was used (Equation (3)). This calculation is based on the approach of Fenton and Karma (1998), who used it to produce a good fit of curves for restitution of action potentials. Application of this method largely prevented overshooting or undershooting at the day-to-night transition. However, simulations of metabolite dynamics using one complete parameter set for day and night still yielded insufficient fit of measured and calculated metabolite levels. This resulted from a characteristic of the Catmull–Rom spline used for interpolations. This spline is a cubic hermite spline that uses two points preceding and two points following a given time point to calculate the value for that time point. Thus, values at the end of the day have a strong impact on the night and vice versa. To eliminate this mathematical artifact, it was necessary to use separate parameter sets for day and night, for which parameters were identified independently.

$$SupportingPoint = \tanh((2/TimeIntervalLength)\, CurrentTime))\; DiffDayNight \quad (3)$$

where *SupportingPoint* is the PS or PR value at the current time point within the interval, $TimeIntervalLength = 0.2$ h, *CurrentTime* is the time point within the interval 0.1 h before and 0.1 h after start of the dark

period minus the starting point of the interval, and *DiffDayNight* is the ΔPS or ΔPR between day and night.

2.6 | Data analysis and statistics

Data evaluation, normalization, visualization and statistics were performed in Microsoft Excel (Microsoft Office version 2010) and the R software (The R Project for Statistical Computing; http://www.r-project.org/).

3 | RESULTS

3.1 | Acclimation to eCO_2

As a first step toward understanding the metabolic processes underlying plant acclimation to eCO_2, conditions were established that allowed verification of eCO_2 acclimation by gas exchange measurements. Plants were grown at 1000 ppm CO_2 for 6 weeks, and during the seventh week NPS rates were compared to those of control plants grown at ambient CO_2 (450 ppm) for 6 weeks and shifted to eCO_2 only 48 h ago. The latter treatment ensured that plants were not in a transitional state between ambient and eCO_2, but did also not yet photosynthetically acclimate to eCO_2. As shown in Table 1, plants acclimated to eCO_2 had diminished NPS. The non-acclimated wild type, Col-0, had an average NPS rate of 132.04 $\mu molg^{-1}$ FW h^{-1}, while acclimated plants showed gas exchange rates of only 90.98 $\mu molg^{-1}$ FW h^{-1}. For the *hpr1-1* mutant, acclimation resulted in photosynthetical activity of 104.96 $\mu molg^{-1}$ FW h^{-1}, and non-acclimated plants showed an activity of 152.78 $\mu molg^{-1}$ FW h^{-1}. While two-way-ANOVA for genotype and treatment revealed a clear effect of acclimation ($p = 0.00491$), NPS of the mutant was not significantly different from wild type under eCO_2. Nevertheless, the *hpr1-1* mutant had a higher respiration than the wild type, indicating higher metabolic activity during the dark phase (see Table S1).

Acclimation to eCO_2 correlated with several changes in primary metabolites (Figure S1). Among soluble sugars (Figure S2), hexoses displayed the strongest effect of acclimation to eCO_2, while sucrose (Suc) remained fairly constant. Fructose (Frc) and glucose (Glc) levels during the light phase declined by trend in acclimated wild type but significantly rose in acclimated *hpr1-1* plants (ANOVA for treatment × genotype, $F_{3,76} = 11.82$, $p = 0.0011$). Thus, the higher Frc concentration of non-acclimated wild type as compared to mutant plants was lost during acclimation. Starch content at the end of the day was not altered in acclimated plants, but was higher in *hpr1-1* as compared to Col-0 (Figure S3). MF accumulated during the light phase and declined in the dark, creating a clear diurnal profile in both genotypes that was more distinct in acclimated plants (Figure 1). These two metabolites were pooled based on the similar behavior reported by Küstner et al. (2019). Although absolute levels sank during acclimation in Col-0 ($p = 0.0435$), diurnal dynamics persisted but declined in the mutant. Citrate (Cit) displayed a diurnal pattern opposite to MF in non-acclimated plants with strongly elevated levels in *hpr1-1* ($p = 9.19e\text{-}11$). The diurnal oscillation was completely lost in acclimated wild type but still visible in the mutant. The non-acclimated *hpr1-1* mutant formed a clearly separated cluster in principal component analysis (PCA) due to accumulation of compounds involved in N-assimilation, such as total AA, nitrate and α-KG (Figure S4). Total AA increased during the day in non-acclimated plants ($r = 0.376$, $p = 0.0002$) and reached very high levels in *hpr1-1* (Figure 2C). Acclimation caused a significant reduction in free AA only in the mutant ($F_{3,284} = 25.8$, $p = 8.4e\text{-}15$). As with Cit, diurnal dynamics decayed in acclimated wild type, but not in the mutant. As shown in Figure 2A,B, Gly and Ser, which were separated from the total AA pool, massively accumulated during the day in *hpr1-1*, but especially Ser levels remained constant after acclimation. Both genotypes had lower nitrate concentrations under eCO_2 ($p = 3.05e\text{-}7$, Figure 2D).

For modeling, enzyme activities of SPS, the hexokinases (fructokinase and glucokinase) and the HPR were considered key enzymes in the pathways for sucrose build-up, sucrose cycling and the photorespiratory salvage pathway, respectively. In the case of HPR, this was done, because this activity discriminates the *hpr1-1* mutant from the wild type. *In vitro* maximum turnover rates were determined to obtain parameter boundaries for the values used in modeling Michaelis–Menten kinetics (Figure S5). Fructokinase showed an increased activity in the non-acclimated *hpr1-1* mutant ($p = 3.77e\text{-}05$). Even though no significant effect could be demonstrated, there was also a tendency to an increased glucokinase activity. The wild type displayed a clearly increased SPS activity for acclimated plants ($p = 0.00977$). This was not the case for *hpr1-1*. Interestingly, no effect except the expected genotype effect was observed for HPR activity.

TABLE 1 Means and standard deviation (SD) of net photosynthesis in $\mu mol/gFW^{-1}$ h^{-1} during light phase for Col-0 and hpr1-1 in either non-acclimated or acclimated state. Measurements were carried out at elevated CO_2 ($n = 12$, 10, 11, and 12)

Genotype	Acclimation	Mean	SD
Col-0	Non-acclimated	132.04	30.94
hpr1-1	Non-acclimated	152.78	37.70
Col-0	Acclimated	90.98	35.22
hpr1-1	Acclimated	104.96	42.74

3.2 | Metabolic changes caused by transfer from ambient CO_2 to eCO_2

To distinguish between the effect of eCO_2 treatment and the acclimation to eCO_2, a set of plants grown at ambient CO_2 was analyzed and compared to plants exposed to eCO_2 for 48 h (Table S2). For the photorespiratory intermediates Gly and Ser a strong decrease was observed following the shift to eCO_2. Thus, photorespiratory intermediates that build up at ambient CO_2 did not persist in non-acclimated plants, indicating formation of a new homeostasis. In addition,

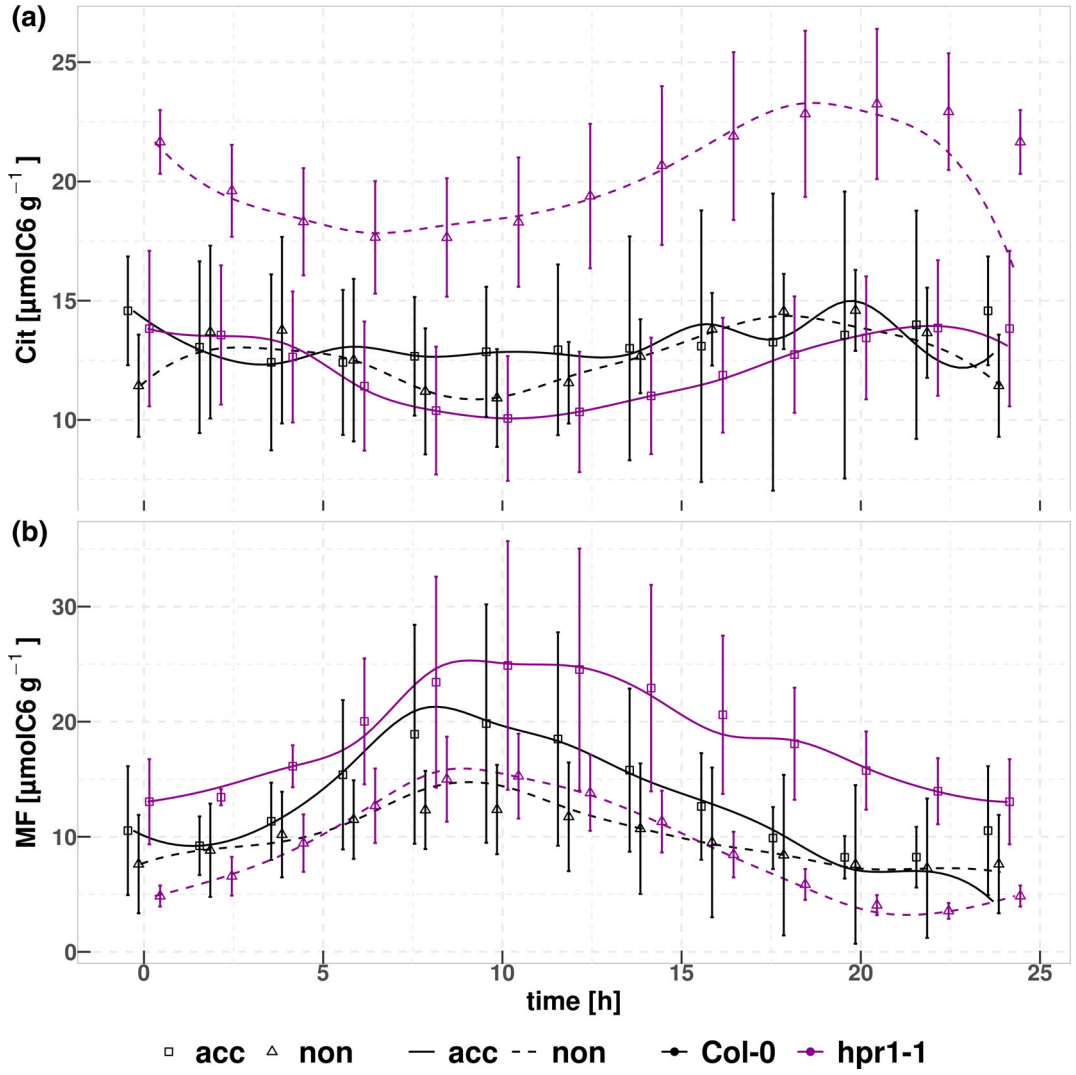

FIGURE 1 Measured values and results of simulations for citrate (Cit) (A) and the malate/fumarate (MF) pool (B). Lines represent the means of 20 simulations. Means of measured values ± standard deviation ($n = 5$) are shown as dots. Light period is from 0 to 8 h. To prevent overlapping, error bars were displaced by 0.25 h

carbonic acids were measured at ambient CO_2 concentrations and plants shifted to eCO_2. For the MF pool similar diurnal dynamics were detected at ambient and eCO_2, although, for the latter at lower absolute concentrations. In contrast, Cit was strongly affected by the eCO_2 treatment. As can also be seen in Figure 1, the Cit pool showed almost no diurnal dynamics under eCO_2 in wild type plants, but was highly dynamic at ambient CO_2 (Table S2). The *hpr1-1* mutant had higher levels than wild type of Cit under ambient as well as eCO_2, but in this case diurnal dynamics persisted in non-acclimated plants and declined only after acclimation (Figure 1).

3.3 | Model construction

For simulating the impact of eCO_2 on interaction of carbon and nitrogen metabolism, a model was set up as described in Figure 3. The exchange of CO_2 with the environment covers the sum of three processes: photosynthetic fixation, PR and mitochondrial respiration. Although mitochondrial respiration can only be measured during the dark phase, it was set as a constant rate over the entire diurnal cycle, because Küstner et al. (2019) have demonstrated that this improves modeling of diurnal metabolite dynamics. Thus, the amount of mitochondrial respiration was added to measured carbon uptake to calculate the flux of primary fixation. This is termed adjusted PS. Like mitochondrial respiration, PR is a process that releases CO_2, thus reducing net carbon uptake. During the light phase, it must therefore also be added to the measured carbon uptake in order to calculate the rate of primary fixation. The adjusted primary fixation was used as input term to form HP, which are connected to the carbohydrates (Suc, Glc, and Frc) in the sucrose-cycling pathway (Küstner et al., 2019; Nägele et al., 2010). In addition, HP were considered as substrate for the synthesis of MF which functioned as a precursor for the Cit/α-KG pool. Cit and α-KG were modeled as one pool, because α-KG is

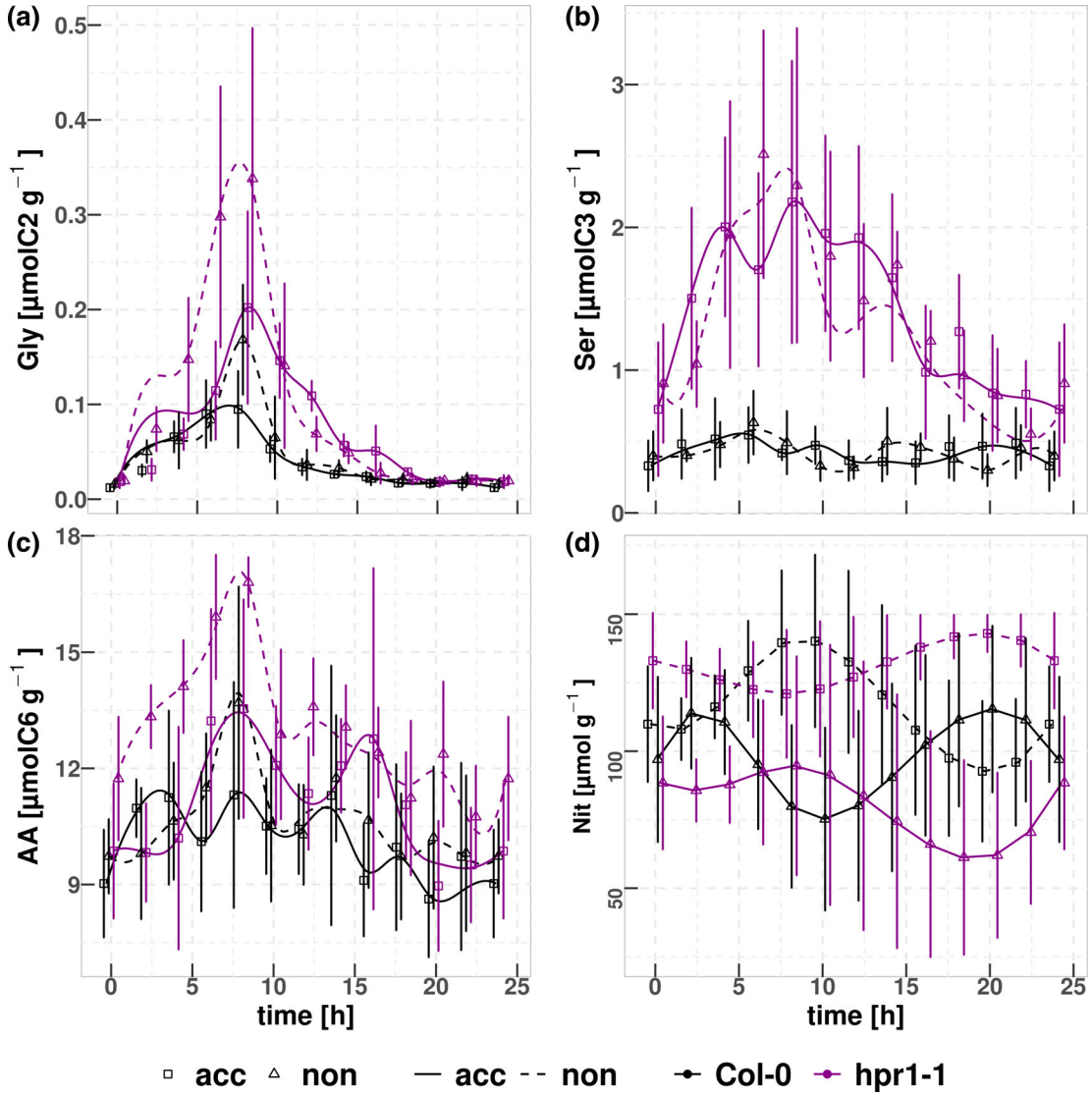

FIGURE 2 Measured values and results of simulations for glycine (Gly) (A), serine (Ser) (B), total amino-acids (AA) (C) and nitrate (Nit) (D). (A–C) Lines represent the means of 20 simulations. Means of measured values ± standard deviation ($n = 5$) are shown as dots. Light period is from 0 to 8 h. To prevent overlapping, error bars were displaced by 0.25 h

mostly generated via isocitrate dehydrogenases (Tcherkez et al., 2017), while transamination reactions, e.g. using glutamate and oxaloacetate for α-KG production, do not contribute significantly (Hodges, 2002). Abadie et al. (2017) have shown that citrate, isocitrate, and α-KG together form the source for Glu production, no matter whether they stem from "old" or recently fixed carbon.

It has been demonstrated that during the light phase α-KG production relies mostly on stored citrate (Tcherkez et al., 2009). However, various modes of the TCA cycle and anaplerotic reactions have been proposed (Hanning & Heldt, 1993; Sweetlove et al., 2010), and thus a connection of the MF and Cit/α-KG pool was allowed also in the light, when phosphoenolpyruvate is used to form oxaloacetate. Phosphoenolpyruvate in our model is part of the HP pool that contains all short-lived intermediates. The MF pool served as substrate for dark respiration. Although this is a simplification of the TCA cycle, it allowed for dissection of Cit/α-KG dynamics, connected to AA metabolism, and energy household.

3.3.1 | PR and C/N interaction at eCO_2

PR activity was calculated according to Sharkey (1988) (Equations (1) and (2)). Values of the CO_2 compensation point (τ^*) for wild type and *hpr1-1* were measured according to Brooks and Farquhar (1985), resulting in a value of 50 ± 10 ppm for Col-0 and 92.5 ± 17.6 ppm for the *hpr1-1* mutant. No significant treatment effect was obtained in our measurements. Because the CO_2 concentration at the carboxylation site is unknown, PR rates were calculated assuming in internal CO_2 concentration of 600 ppm, following the suggestion of Sharkey (1988). A parameter α was introduced into the rate equation

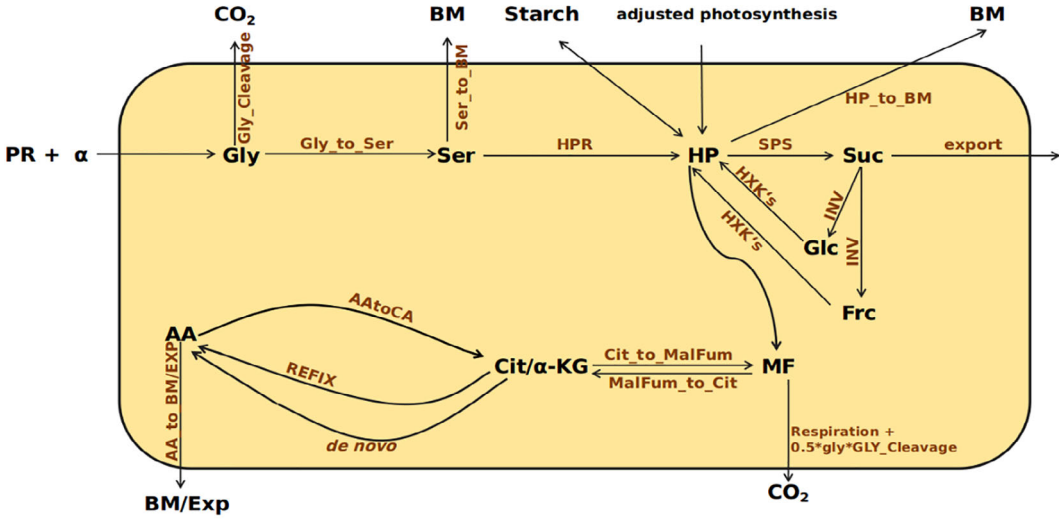

FIGURE 3 Schematic representation of the ODE-model used for simulations. States within the system-boundaries: glycine (Gly), serine (Ser), amino acids (AA), hexosephosphates (HP), sucrose (Suc), glucose (Glc), fructose (Frc), citrate (Cit), α-Ketoglutarate (α-KG), malate, and fumarate (MF). States outside of the system: biomass (BM), starch (Starch), and export (Exp). Constant fluxes across the system boundaries: net photosynthesis (adjusted photosynthesis), photorespiration (PR). A Michaelis–Menten kinetic was used for sucrose-phosphate-synthase (SPS), hexokinases (HXK's = fructokinase and glucokinase), invertase (INV), and the hydroxypyruvate-reductase (HPR). The remaining statements are modeled as mass action kinetics

for PR in order to allow flux through the salvage pathway in the absence of NPS, i.e. during the dark phase. Boundaries for α were set between 0 and 5 for all simulations. Inclusion of α substantially improved simulation of dynamics for Gly and Ser during the night, especially for the *hpr1-1* mutant, where metabolism of both AAs was distinctly extended into the dark phase (Figure 2A,B). A striking feature of the *hpr1-1* mutant was an altered ratio of PS to dark respiration; the latter being strongly elevated (Table S1). According to Sharkey (1988), this results in calculating a higher rate of PR, which, due to the mutant phenotype, causes accumulation of Gly and Ser, because PR flux is reduced in *hpr1-1*. This was confirmed by the metabolite data (Figure 2) and caused a higher value of α during the dark phase in this mutant.

It should be emphasized that the model shown in Figure 3 is a pure carbon metabolism model, which, however, allows for calculation of N fluxes at the interconversions of carboxylates and AA. While PR provides the carbon contained in the Gly pool, the nitrogen is donated by either Glu or Ser. Therefore, the HPR rate, which releases N, was subtracted from PR in order to take account of the N delivered by Ser. The remaining N comes from Glu, which in our model is contained in the AA pool. The corresponding rate from AA to Cit/α-KG is called AAtoCA (Figure 3 and Equation (4)). The stoichiometric factor 0.813 takes into account that the AA pool has 1.23 μmol N per μmol C6.

$$AAtoCA = [(PR + \alpha) - HPR]\,0.813\,AA \tag{4}$$

where *AAtoCA* is the flux from AA pool into the Cit/α-KG pool, *AA* is the current AA concentration, *PR* is the PR, α is the factor described above, and *HPR* is the current value of the HPR activity.

During the reaction from Gly to Ser, one N is released in the form of ammonia. This has to be re-fixed. The carbon skeleton is α-KG which is represented by the Cit/α-KG pool. Therefore, a reaction called REFIX was introduced into the model (Figure 3 and Equation (5)). REFIX represents the rate of Cit/α-KG to AA conversion and is proportional to the rate from Gly to Ser. The factor 4.878 is the C/N ratio of the AA pool and is used to transform the N1 flux into a C6 flux. Note that the parameters gly_cleavage and gly_to_ser were set to the same value in order to account for the spatial proximity of glycine cleavage enzyme and the serine-hydroxymethyl-transferase (Douce et al., 2001).

$$REFIX = gly\,gly\_cleavage\,4.878 \tag{5}$$

where *REFIX* is the flux from Cit/α-KG pool into the AA pool, *gly* is the current Gly concentration and *gly_cleavage* is the rate constant. Thus, only the parameters for de novo N-assimilation needed to be optimized according to the dynamics of AA and Cit/α-KG cycling.

As can be seen from Equations (4) and (5), the fluxes between AA and the Cit/α-KG pool that arise from PR are only depending on Ser and Gly concentrations. Besides these, a flux from the Cit/α-KG pool into the AA pool, which is independent of PR activity but relies on the α-KG concentration as substrate, results from *de novo* N assimilation. Thus, by identifying the parameters for Equations (4) and (5), it is possible to differentiate between *refixation* of ammonia and *de novo* N-fixation.

3.4 | Simulated fluxes at eCO_2

Simulations of metabolite dynamics matched measured values with a maximal deviation of 8.2% per time point and state and remained

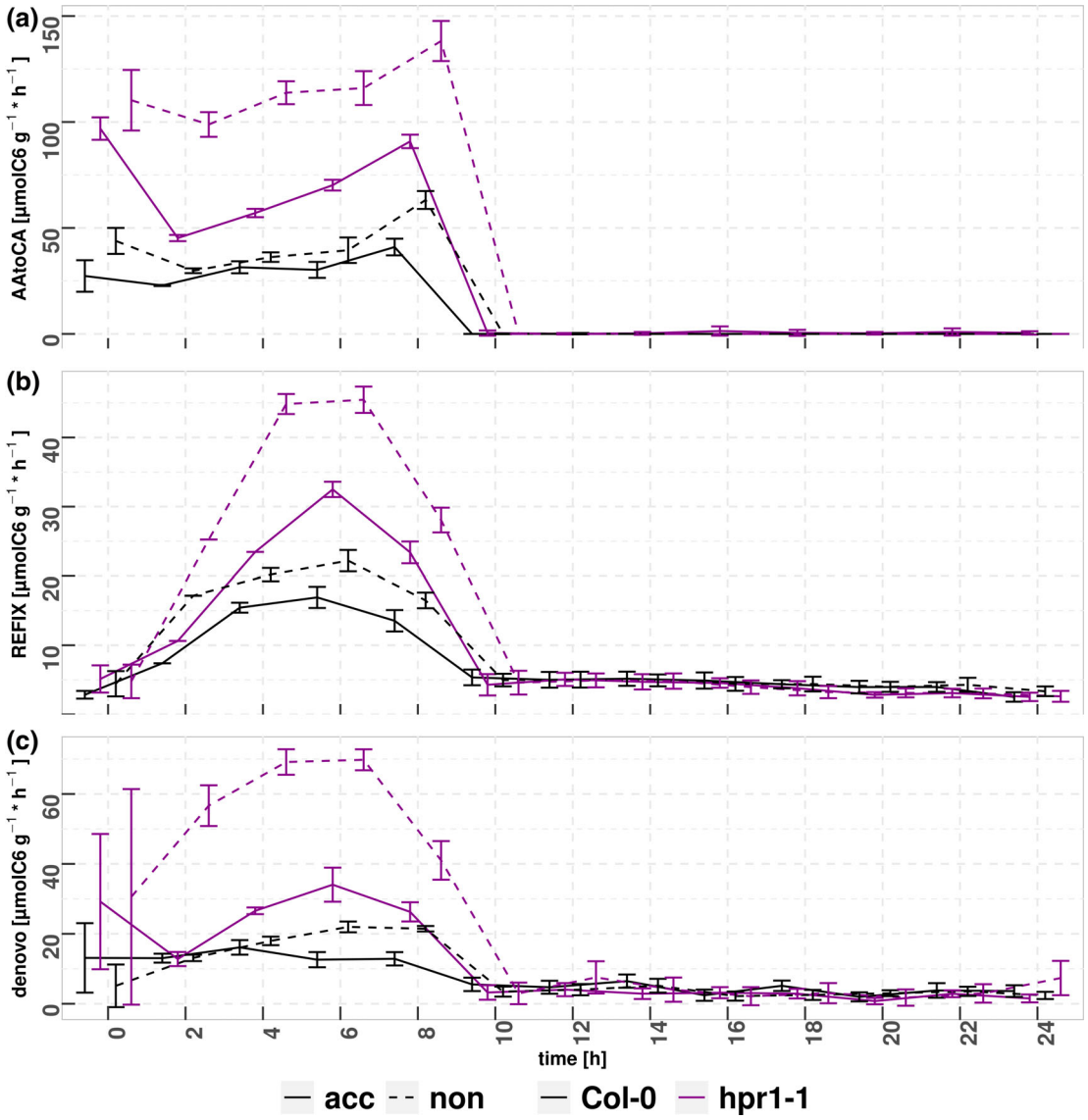

FIGURE 4 Flux calculations for interconversion of total amino acids and the Cit/α-KG pool. AAtoCA is the amino acid consumption for Gly synthesis (A). REFIX is the refixation of N produced by glycine-cleavage enzyme (B). Denovo is the de novo fixation of N (C). Error bars depict SD simulations ($n = 20$). Light period is from 0 to 8 h. All values are evaluated every 2 h. To prevent overlapping of error bars calculated for identical time points, bars were displaced by 0.25 h

within the standard deviation with few exceptions (Figures 1, 2, and S2). Although the default error calculated by the *paropt* algorithm is the sum of absolute differences between measured and simulated states, a relative error was calculated by the cost function in order to improve results especially for low concentrated metabolites Hence, it was possible to optimize very small (e.g. Gly) as well as large states (e.g. AA) at the same time with similar accuracy. Based on substrate concentrations and the identified parameters, flux rates at specific time-points could be calculated. Figure 4 and Table 2 show the calculated fluxes. As expected, fluxes in the AA-to-Cit/α-KG cycle, which are in part dependent on PR, are significantly increased for the non-acclimated plants (Table 2).

The rate of Gly accumulation in the light was about 1.5-fold higher in non-acclimated versus acclimated Col-0 and about doubled

TABLE 2 Means of 20 simulations for the fluxes, 6 h after light-on, in µmol C6 gFW^{-1} h^{-1}. Col-0 acclimated (C.acc), Col-0 non-acclimated (C.non), *hpr1-1* acclimated (h.acc), and *hpr1-1* non-acclimated (h.non). *AAtoCA* is the amino-acid consumption for synthesis of Gly. *REFIX* is the refixation of N produced by glycine-cleavage enzyme. *denovo* is the de novo fixation of N. Letters indicate the results of Tukey's HSD following two-way ANOVA for genotype × treatment. Groups sharing the same letters are not significantly different ($p \leq 0.05$; $n = 20$)

Fluxes	C.acc	C.non	h.acc	h.non
AAtoCA	30.22^{d}	39.49^{c}	70.19^{b}	116.00^{a}
REFIX	16.92^{d}	22.19^{c}	32.49^{b}	45.45^{a}
denovo	12.60^{d}	21.98^{c}	34.06^{b}	69.77^{a}

in non-acclimated *hpr1-1*. These higher rates, in turn, stimulated higher turnover of the AA-to-Cit/α-KG cycle. Simulations revealed that this supported a significantly increased *de novo* N assimilation using α-KG as substrate, while already fixed N was deposited as Gly and, at least in the mutant, also as Ser (Figure 2).

As a consequence of the mutation, HPR activity was strongly reduced in *hpr1-1* plants. Thus, the flux from Ser to HP was limited, which restricted the N flux from Ser to Gly. This in turn caused more AA to be used for Gly formation with the effect of elevated *de novo* N assimilation in the mutant (Figure 4 and Table 2).

4 | DISCUSSION

4.1 | Metabolic changes during acclimation to eCO_2

Three sets of plants were analyzed in this study—plants grown at ambient CO_2 concentration as well as plants either continuously grown at eCO_2 or shifted from ambient to eCO_2 for 48 h. Comparison of plants grown under ambient versus eCO_2 revealed that the most significant changes in the PR intermediates Gly and Ser completed within the first 2 days at eCO_2, while changes in Cit metabolism took longer to reach a new homeostasis. Continuous growth at eCO_2 resulted in a reduction of photosynthetic activity by about 20% in wild type and 30% in the *hpr1-1* mutant, thus clearly demonstrating acclimation of PS to eCO_2 within 44 days of exposure. Similar effects, expressed as reduced rate of RUBISCO carboxylation (V_{cmax}), have been reported by Jauregui et al. (2018) after 28 days at eCO_2 under long day conditions. In this study, the extent of acclimation coincided with the amount of foliar starch that appeared to negatively affect RUBISCO performance. Under the short day conditions applied in the present study, no difference in starch content was observed for acclimated and non-acclimated plants, arguing against a direct effect of the starch content. Interestingly, Jauregui et al. found dependence of acclimation on the source of N fertilization: while plants fertilized with nitrate did show acclimation, plants fertilized with a mixture of ammonium and nitrate retained higher photosynthetic rates under eCO_2 over extended periods of time (Jauregui et al., 2015), thus indicating an interaction of acclimation with N fixation. Because the most important source of ammonium during the light period is PR, we recorded diurnal profiles of PR intermediates under ambient and eCO_2 and found the typical diurnal profiles, i.e. a light-dependent accumulation of Gly and Ser in Col-0 and *hpr1-1* even at eCO_2. As already reported by Timm et al. (2008), amplitudes were increased in the *hpr1-1* mutant. This proved that PR still operates under the condition of a doubled atmospheric CO_2 concentration and is in agreement with data reported by Sage (1994). In various studies involving PR mutants, CO_2 concentrations of 3000 ppm and even higher were used in order to avoid oxygenation of RUBISCO (e.g. Timm et al., 2010). In the present study, 1000 ppm were applied to substantially reduce, but not eliminate, PR in both genotypes (Table S2 and Figure 2), because otherwise the impact of perturbed PR on acclimation to eCO_2 could not be investigated. With PR operating in both genotypes at a reduced rate in eCO_2 the *hpr1-1* mutant still showed increased Gly and Ser levels when compared to the wild type, and thus the effect of different PR fluxes could be examined. This revealed that diurnal dynamics of Cit persisted in non-acclimated *hpr1-1* plants, but dynamics completely declined in wild type and acclimated *hpr1-1*. The decreased diurnal dynamics of Cit reflect reduced consumption of α-KG for ammonia re-fixation under eCO_2, and this was strongly delayed in the *hpr1-1* mutant. Gauthier et al. (2010) showed that α-KG is produced from carbon that was stored during the previous night. The fact that the MF pool retained diurnal dynamics in both genotypes under eCO_2, although at reduced absolute levels (Table S2), while dynamics declined for Cit, is strong evidence that the MF and Cit pool are independent of each other. As demonstrated by Tcherkez et al. (2009), α-KG predominantly derives from "old" Cit, while malate production depends on phosphoenolpyruvate. However, the simulations presented here do not finally disclose at which mode the TCA cycle operates during the light phase (Sweetlove et al., 2010).

Even though PR was not stalled at 1000 ppm of CO_2, its contribution to gas exchange was substantially reduced. With the rate of the Gly accumulation in the light taken as an indicator of RUBISCO oxygenation, PR was reduced by about 35% in Col-0 and nearly 50% in the *hpr1-1* mutant. A central question addressed in this study was whether reduced PR, and the concomitant reduction in ammonium availability, could have caused photosynthetic acclimation as suggested by the data of Jauregui et al. (2015). Because PR and PS are interlinked (Sharkey, 1988), it is difficult to separate cause and effect. However, comparison of the *hpr1-1* mutant with Col-0 wild type revealed important details. If we assume that the ratio of carboxylation and oxygenation of RUBISCO is not affected by the *hpr1-1* mutation, the much stronger reduction of daily Gly accumulation after long-term exposure to eCO_2 in *hpr1-1* must be attributed to an altered flux through the PR salvage pathway. With this flux and an independent recording of photosynthetic activity, a ratio of PR to NPS can be calculated, which is higher in non-acclimated plants (Col-0 ca. 17% and *hpr1-1* ca. 26%) even though both sets of plants were analyzed in an atmosphere with identical CO_2 concentration. This implies a decline of PR flux relative to NPS during acclimation to eCO_2, and this decline was supported by our flux simulations that identified reduced PR fluxes in acclimated plants. There are two possible explanations for the higher PR flux in non-acclimated plants. Either the higher PS in non-acclimated plants caused a local depletion of CO_2 at the carboxylation site that could not be compensated by CO_2 diffusion within the leaf tissue, or metabolic and/or enzymatic alterations in acclimated plants limited the capacity for PR.

Sage (1994) reported that for internal CO_2 concentrations between 200 and about 550 ppm, PS is limited by the regeneration of ribulose-1,5-bisphosphate and, thus, responsive to changes in the CO_2-to-O_2 ratio, while for higher internal CO_2 (C_i) concentrations, PS becomes limited by P_i regeneration and is than unaffected by changes in C_i. Given that C_i is about 600 ppm under the conditions of eCO_2 applied here, local depletion of CO_2 at the carboxylation site becomes unlikely. In contrast, however, some of the metabolite changes

observed during acclimation favor a metabolic limitation of PR. Acclimated Col-0 plants had a reduced ratio of sugars versus carboxylic acids during the light phase, indicating a metabolic shift toward TCA cycle intermediates, which is indicative of a C-limited metabolic state.

An increase in carboxylic acids, especially fumarate and citrate, and a concomitant decline in the sugar-to-carboxylate ratio during the light phase at eCO_2 was also observed by Watanabe et al. (2014) for Arabidopsis seedlings grown on artificial medium for 20 days. Seedlings showed a higher CO_2 efflux rate at eCO_2, resulting from the use of carboxylates instead of sugars for respiration. The authors calculated a higher cost for ATP production at eCO_2, which they related to higher energy demand for carbohydrate export to the roots (Watanabe et al., 2014). However, they also found higher rates of AA production that could have stimulated ATP consumption. This was not observed in our study, where the total AA pool (not containing Gly and Ser) declined and nitrate levels were lowered after prolonged exposure to eCO_2.

In acclimated soil grown plants, transamination of glyoxylate by glutamate could have become limiting due to the decrease in the AA pool. This would cause a decline in PR flux and, thus, a depletion of Calvin–Benson cycle intermediates, because the regeneration of glycerate from Ser would slow down. The apparent stimulation of flux into the TCA cycle could thus be considered a compensatory measure to stimulate AA synthesis or may simply reflect reduced buildup of sugars because of detracted export of triose-phosphates from the plastids that resulted from reduced replenishment by the PR pathway. This was especially obvious in *hpr1-1*, which, due to the mutation, has a lower PR capacity than Col-0.

This implies that the capacity of the PR and the PS activity are balanced in order to prevent accumulation of the toxic intermediates 2-PG, glycolate, and glyoxylate. While this is physiologically reasonable, the question remains, why PR flux is reduced in acclimated plants.

4.2 | N assimilation

To determine whether acclimation of PS and reduced PR are causally linked, we developed a mechanistic model and identified kinetic parameters that were used for flux calculation of C and N fixation (Figures 3 and 4). For simulations, the upper boundaries for *de novo* N fixation were set to lower values during the night. The physiological background for this is high demand for reducing equivalents that are generated during PS in the light period (Farré & Weise, 2012; Gibon et al., 2006). Simulations of metabolite dynamics over a full diurnal cycle revealed an impact of PR on *de novo* N assimilation. Remarkably, non-acclimated plants shifted to high CO_2 for not more than 48 h showed higher *de novo* N fixation as compared to acclimated plants (Figure 4). Hence, long-term exposure to high CO_2 reduced N acquisition, resulting in an increased C/N ratio. This has also been observed by Jauregui et al. (2016) and coincided with halving of the foliar ammonium content, while nitrate content remained unchanged.

While the pathways of PS, PR, and N fixation involve various subcellular compartments, compartmentalization was not included in the model, because metabolite measurements were not subcellulary resolved. Thus, the reported concentrations of Gly and Ser in whole cell extracts very likely underestimate the local concentrations in mitochondria and peroxisomes. In case of the local concentration were higher than disclosed here, fluxes would be larger, resulting in higher turnover between Cit and AA. While this would change the absolute fluxes, relations reported for genotypes and treatments would not be affected. Our simulations indicated that at eCO_2 refixation of ammonium released during Gly cleavage was low due to low PR activity (Figure 4 and Table 2). Thus, under eCO_2, only a small amount of N is deposited in the form of Gly and Ser, two AAs with very low carbon content. An important consequence of reduced Gly turnover in the peroxisome is a low rate of glutamate transamination and, therefore, release of α-KG becomes restricted (Bloom et al., 2020). Because α-KG is the prime carbon skeleton for *de novo* AA production, this could negatively affect *de novo* N acquisition, thus leading to an elevated C/N ratio. Hodges (2002) reported that provision of α-KG by mitochondrial isocitrate-dehydrogenase should be inhibited in the light due to the production of NADH. Alternatively, α-KG could be produced by aspartate transaminase, but this would not create a net flux of N into the AA pool. Thus, deposition of already fixed N in AAs with low C content could be essential for effective *de novo* N assimilation. This concept puts PR into the role of a storage pathway for assimilated N during the light phase, when, because of a non-cyclic TCA (Sweetlove et al., 2010), provision of carbon for AA synthesis is limited. Gauthier et al. (2010) pointed out that C stored during the previous night has to be re-mobilized in order to supply α-KG for *de novo* N assimilation. Our data substantiates this finding by demonstrating that N present within the α-KG family of AA can temporarily be stored in the PR pathway in order to increase α-KG availability for *de novo* N assimilation. This is also supported by the finding that the non-acclimated *hpr1-1* mutant, which stores large amounts of Gly and Ser, showed the highest *de novo* fixation of N and, in accordance with that, had elevated total AA content.

It should also be mentioned that eCO_2 may negatively affect N assimilation by additional mechanisms, such as the inhibited transport of nitrite into the plastids and inhibition of succinate dehydrogenase, thus lowering energy provision for N assimilation (Asensio et al., 2015). These effects cannot be addressed in the mechanistic model presented here and may potentially add to the inhibition of *de novo* N assimilation. However, Bloom et al. (2014) showed that the impact of eCO_2 on nitrate assimilation is the most important effect, thus emphasizing the importance of the provision of carbon skeletons for N assimilation and the storage of N in the PR pathway.

Besides the N storage function, reduced PR turnover could also affect malate availability in the cytosol. As proposed by Bloom et al. (2010) and Rachmilevitch et al. (2004), the cutback in ammonium release due to lower PR rates might cause decreased export of malate from the plastids that are exchanged against α-KG as part of the malate shuttle. Bloom et al. (1989) pointed to the high demand for electrons produced by PS in the assimilation of nitrate. Malate in the

cytosol could be required to produce NADH as substrate for the nitrate-reductase. Long-term exposure to eCO_2 might therefore cause a shift in the C/N based on a shortage of NADH in the cytosol. In the *hpr1-1* mutant, however, large amounts of NADH are produced by the glycine-cleavage enzyme (Leegood et al., 1995), and this could relate to the high AA levels in this mutant. An unsolved question regarding PR as promoter of malate transport into the cytosol and its use for NADH production remains with its function also in the exchange against glutamate produced in the plastids (Nunes-Nesi et al., 2010; Renné et al., 2003). This transport is essential for providing glutamate for the transamination that converts glyoxylate into Gly. Thus, the malate transport hypothesis may not be able to fully explain the benefits of PR for N assimilation.

4.3 | Metabolic dysfunctions in the *hpr1-1* mutant at ambient CO_2 concentrations

The design of the current study involved plants exposed to eCO_2 either long-term or short-term to uncover mechanisms of eCO_2 acclimation. Thus, the metabolic effects of the *hpr1-1* mutation under ambient CO_2 are not immediately visible. However, considering literature data and metabolic features of non-acclimated *hpr1-1* plants, some peculiarities of the mutant became obvious. The *hpr1-1* mutant had high AA as well as starch and citrate levels, but nevertheless produced less biomass. Timm et al. (2010) and Li et al. (2019) described a chlorotic phenotype, and this was attributed to a possible intoxication by glycolate, glyoxylate or 2-phospho-glycolate (Dellero et al., 2016). After a 48 h shift to eCO_2, we observed reduced hexose levels and higher dark respiration in *hpr1-1* as compared to wild type, as well as increased hexokinase activity, indicating enhanced catabolism. This is supported by low MF levels and an accumulation of α-KG especially during the night. While it is very likely that this relates to processing of the high Gly and Ser stock that piled up under ambient CO_2 (Table S2), it also demonstrates a metabolic shift from sugar to carboxylate metabolism. This is accompanied by strongly elevated phosphate levels, which are inhibitory to SPS and cytosolic fructose-bisphosphate phosphatase via stimulation of fructose-6-phosphate-2-kinase. It could thus be envisaged that *hpr1-1* is limited in carbohydrate supply and, hence, in provision of cell wall material for growth. However, our flux calculations also point to an additional problem. Turnover of Gly was strongly expanded into the night in *hpr1-1* (Figure 2) and may thus fall into a period of low abundance of glutamine synthetase 2 (GS2), which is responsible for re-fixation of ammonia. Seabra et al. (2013) have shown that GS2 abundance is low during the night, and although posttranslational regulation might compensate for low protein abundance under normal conditions, this may not suffice for the high Gly levels present in *hpr1-1*, which may then lead to accumulation of toxic levels of ammonia. However, it cannot be excluded that non-enzymatic decarboxylation of hydroxypyruvate occurs in *hpr1-1*, which, as suggested by Cousins et al. (2011), would lead to intoxication by glycolate.

5 | CONCLUSIONS

Our model is capable of describing the fluxes between the AA and Cit/α-KG pools, thus allowing the assessment of N re-fixation and *de novo* assimilation. Simulations for conditions of varied PR activity revealed that the storage capacity of the PR pathway for N in the form of Gly and Ser is correlated with the level of *de novo* N assimilation. Reduced PR activity after long-term eCO_2 exposure therefore appears to at least contribute to photosynthetic acclimation to eCO_2 by creating a C/N imbalance.

ACKNOWLEDGMENTS

The authors would like to thank Prof Hermann Bauwe for a generous gift of seeds of the *hpr1-1* mutant used in this study. Nadja Beuttenmüller and Annika Allinger are acknowledged for expert plant cultivation. K.K. received a scholarship "Landesgraduiertenförderung (LGF)" of the Federal State of Baden-Wuerttemberg (Germany). Konrad Krämer holds a stipend by the county of Baden Württemberg.

Open access funding enabled and organized by Projekt DEAL.

AUTHOR CONTRIBUTIONS

Konrad Krämer: Designed the study, conducted experiments, developed the model, and wrote the manuscript. Gabi Kepp, Simon Stutz, and Judith Brock: Conducted experiments. Arnd G. Heyer: Designed the study and wrote the manuscript.

DATA AVAILABILITY STATEMENT

Raw data can be made available by the authors upon request.

ORCID

Arnd G. Heyer https://orcid.org/0000-0003-2074-3234

REFERENCES

Abadie, C., Lalande, J., Limami, A.M. & Tcherkez, G. (2021) Non-targeted 13C metabolite analysis demonstrates broad re-orchestration of leaf metabolism when gas exchange conditions vary. *Plant, Cell & Environment*, 44(2), 445–457. https://doi.org/10.1111/pce.13940

Abadie, C., Lothier, J., Boex-Fontvieille, E., Carroll, A. & Tcherkez, G (2017) Direct assessment of the metabolic origin of carbon atoms in glutamate from illuminated leaves using 13C-NMR. *New Phytol*, 216, 1079–1089. https://doi.org/10.1111/nph.14719

Ainsworth, E. & Rogers, A. (2007) The response of photosynthesis and stomatal conductance to rising [CO2]: mechanisms and environmental interactions. *Plant, Cell & Environment*, 30(3), 258–270. https://doi.org/10.1111/j.1365-3040.2007.01641.x

Akman, D., Akman, O. & Schaefer, E. (2018) Parameter estimation in ordinary differential equations modeling via particle swarm optimization. *Journal of Applied Mathematics*, 2018, 1–9. https://doi.org/10.1155/2018/9160793

Asensio, J.S.R., Rachmilevitch, S. & Bloom, A.J. (2015) Responses of Arabidopsis and wheat to rising CO2 depend on nitrogen source and nighttime CO2 levels. *Plant Physiology*, 168(1), 156–163. https://doi.org/10.1104/pp.15.00110

Biernath, C., Bittner, S., Klein, C., Gayler, S., Hentschel, R., Hoffmann, P. et al. (2013) Modeling acclimation of leaf photosynthesis to atmospheric CO2 enrichment. *European Journal of Agronomy*, 48, 74–87. https://doi.org/10.1016/j.eja.2013.02.008

Bloom, A.J., Burger, M., Kimball, B.A. & Pinter, P.J. (2014) Nitrate assimilation is inhibited by elevated CO2 in field-grown wheat. *Nature Climate Change*, 4(6), 477–480. https://doi.org/10.1038/nclimate2183

Bloom, A.J., Burger, M., Rubio Asensio, J.S. & Cousins, A.B. (2010) Carbon dioxide enrichment inhibits nitrate assimilation in wheat and Arabidopsis. *Science*, 328(May), 899–904.

Bloom, A.J., Caldwell, R.M., Finazzo, J., Warner, R.L. & Weissbart, J. (1989) Oxygen and carbon dioxide fluxes from barley shoots depend on nitrate assimilation. *Plant Physiology*, 91(1), 352–356. https://doi.org/10.1104/pp.91.1.352

Bloom, A.J., Kasemsap, P. & Rubio-Asensio, J.S. (2020) Rising atmospheric CO2 concentration inhibits nitrate assimilation in shoots but enhances it in roots of C3 plants. *Physiologia Plantarum*, 168(4), 963–972. https://doi.org/10.1111/ppl.13040

Brooks, A. & Farquhar, G.D. (1985) Effect of temperature on the CO2/O2 specificity of ribulose-1,5-bisphosphate carboxylase/oxygenase and the rate of respiration in the light the light—estimates from gas-exchange measurements on spinach. *Planta*, 165(3), 397–406. https://doi.org/10.1007/BF00392238

Chen, G.Y., Yong, Z.H., Liao, Y., Zhang, D.Y., Chen, Y., Zhang, H.B. et al. (2005) Photosynthetic acclimation in rice leaves to free-air CO2 enrichment related to both ribulose-1,5-bisphosphate carboxylation limitation and ribulose-1,5-bisphosphate regeneration limitation. *Plant and Cell Physiology*, 46(7), 1036–1045. https://doi.org/10.1093/pcp/pci113

Cheng, S.H., Moore, B. & Seemann, J.R. (1998) Effects of short- and long-term elevated CO2 on the expression of ribulose-1,5-bisphosphate carboxylase/oxygenase genes and carbohydrate accumulation in leaves of *Arabidopsis thaliana* (L.) Heynh. *Plant Physiology*, 116(2), 715–723. https://doi.org/10.1104/pp.116.2.715

Cousins, A.B., Walker, B.J. & Pracharoenwattana, I. (2011) Peroxisomal hydroxypyruvate reductase is not essential for photorespiration in Arabidopsis but its absence causes an increase in the stoichiometry of photorespiratory CO2 release. *Photosynth Res*, 108, 91. https://doi.org/10.1007/s11120-011-9651-3

Dabu, X., Li, S., Cai, Z., Ge, T. & Hai, M. (2019) The effect of potassium on photosynthetic acclimation in cucumber during CO2 enrichment. *Photosynthetica*, 57(2), 640–645. https://doi.org/10.32615/ps.2019.073

Dellero, Y., Jossier, M., Schmitz, J., Maurino, V.G. & Hodges, M. (2016) Photorespiratory glycolate – glyoxylate metabolism. *Journal of Experimental Botany*, 67(10), 3041–3052. https://doi.org/10.1093/jxb/erw090

Douce, R., Bourguignon, J., Neuburger, M. & Rébeillé, F. (2001) The glycine decarboxylase system: a fascinating complex. *Trends in Plant Science*, 6(4), 167–176. https://doi.org/10.1016/S1360-1385(01)01892-1

Farré, E.M. & Weise, S.E. (2012) The interactions between the circadian clock and primary metabolism. *Current Opinion in Plant Biology*, 15(3), 293–300. https://doi.org/10.1016/j.pbi.2012.01.013

Fenton, F. & Karma, A. (1998) Erratum: "vortex dynamics in three-dimensional continuous myocardium with fiber rotation: filament instability and fibrillation" [Chaos 8, 20–47 (1998)]. *Chaos*, 8(4), 879–879. https://doi.org/10.1063/1.166374

Bauwe, H. (2017) Measurement of enzyme activities. In: Fernie, A., Bauwe, H. & Weber, A., *Photorespiration. Methods and Protocols*, Vol. 1653. New York, NY, U.S.A.: Humana Press. https://doi.org/10.1007/978-1-4939-7225-8

Gámez, A.L., Vicente, R., Sanchez-Bragado, R., Jauregui, I., Morcuende, R., Goicoechea, N. et al. (2020) Differential flag leaf and ear photosynthetic performance under elevated (CO2) conditions during grain filling period in durum wheat. *Frontiers in Plant Science*, 11(December), 1–12. https://doi.org/10.3389/fpls.2020.587958

Gauthier, P.P.G., Bligny, R., Gout, E., Mahé, A., Nogués, S., Hodges, M. et al. (2010) In folio isotopic tracing demonstrates that nitrogen assimilation into glutamate is mostly independent from current CO2 assimilation in illuminated leaves of *Brassica napus*. *New Phytologist*, 185(4), 988–999. https://doi.org/10.1111/j.1469-8137.2009.03130.x

Gibon, Y., Usadel, B., Blaesing, O.E., Kamlage, B., Hoehne, M., Trethewey, R. et al. (2006) Integration of metabolite with transcript and enzyme activity profiling during diurnal cycles in *Arabidopsis rosettes*. *Genome Biology*, 7(8), R76. https://doi.org/10.1186/gb-2006-7-8-r76

Gifford, R.M., Barrett, D.J. & Lutze, J.L. (2000) The effects of elevated [CO2] on the C:N and C:P mass ratios of plant tissues. *Plant and Soil*, 224(1), 1–14. https://doi.org/10.1023/A:1004790612630

Griffin, K.L. & Seemann, J.R. (1996) Plants, CO2 and photosynthesis in the 21st century. *Chemistry and Biology*, 3(4), 245–254. https://doi.org/10.1016/S1074-5521(96)90104-0

Gutiérrez, D., Morcuende, R., Del Pozo, A., Martínez-Carrasco, R. & Pérez, P. (2013) Involvement of nitrogen and cytokinins in photosynthetic acclimation to elevated CO2 of spring wheat. *Journal of Plant Physiology*, 170(15), 1337–1343. https://doi.org/10.1016/j.jplph.2013.05.006

Hanning, I. & Heldt, H.W. (1993) On the function of mitochondrial metabolism during photosynthesis in spinach (*Spinacia oleracea* L.) leaves. Partitioning between respiration and export of redox equivalents and precursors for nitrate assimilation products. *Plant Physiology*, 103(4), 1147–1154. https://doi.org/10.1104/pp.103.4.1147

Hindmarsh, A.C., Brown, P.N., Grant, K.E., Lee, S.L., Serban, R., Shumaker, D.E. et al. (2005) SUNDIALS: suite of nonlinear and differential/algebraic equation solvers. *ACM Transactions on Mathematical Software*, 31(3), 363–396. https://doi.org/10.1145/1089014.1089020

Hodges, M. (2002) Enzyme redundancy and the importance of 2-oxoglutarate in plant ammonium assimilation. *Journal of Experimental Botany*, 53(370), 905–916. https://doi.org/10.1093/jexbot/53.370.905

IPCC. (2014) Summary for policymakers. Climate change 2014: mitigation of climate change. Contribution of Working Group III to the Fifth Assessment Report of the Intergovernmental Panel on Climate Change. https://doi.org/10.1017/CBO9781107415324

Jauregui, I., Aparicio-Tejo, P.M., Avila, C., Cañas, R., Sakalauskiene, S. & Aranjuelo, I. (2016) Root-shoot interactions explain the reduction of leaf mineral content in Arabidopsis plants grown under elevated [CO2] conditions. *Physiologia Plantarum*, 158(1), 65–79. https://doi.org/10.1111/ppl.12417

Jauregui, I., Aparicio-Tejo, P.M., Avila, C., Rueda-López, M. & Aranjuelo, I. (2015) Root and shoot performance of *Arabidopsis thaliana* exposed to elevated CO2: a physiologic, metabolic and transcriptomic response. *Journal of Plant Physiology*, 189, 65–76. https://doi.org/10.1016/j.jplph.2015.09.012

Jauregui, I., Pozueta-Romero, J., Cordoba, J., Avice, J.-C., Aparicio-Tejo, P.M., Baroja-Fernández, E. et al. (2018) Unraveling the role of transient starch in the response of Arabidopsis to elevated CO2 under long-day conditions. *Environmental and Experimental Botany*, 155, 1–27.

Kanemoto, K., Yamashita, Y., Ozawa, T., Imanishi, N., Nguyen, N.T., Suwa, R. et al. (2009) Photosynthetic acclimation to elevated CO2 is dependent on N partitioning and transpiration in soybean. *Plant Science*, 177(5), 398–403. https://doi.org/10.1016/j.plantsci.2009.06.017

Keys, A.J. (2006) The re-assimilation of ammonia produced by photorespiration and the nitrogen economy of C3 higher plants. *Photosynthesis Research*, 87(2), 165–175. https://doi.org/10.1007/s11120-005-9024-x

Kizildeniz, T., Pascual, I., Irigoyen, J.J. & Morales, F. (2021) Future CO2, warming and water deficit impact white and red Tempranillo grapevine: photosynthetic acclimation to elevated CO2 and biomass allocation. *Physiologia Plantarum*, 172(3), 1779–1794. https://doi.org/10.1111/ppl.13388

Krämer, K., Krämer, J., & Heyer, A. (2020). Paropt: parameter optimizing of ODE-systems.

Kuehny, J.S., Peet, M.M., Nelson, P.V. & Willits, D.H. (1991) Nutrient dilution by starch in CO2-enriched chrysanthemum. *Journal of Experimental Botany*, 42(6), 711–716. https://doi.org/10.1093/jxb/42.6.711

Küstner, L., Nägele, T. & Heyer, A.G. (2019) Mathematical modeling of diurnal patterns of carbon allocation to shoot and root in *Arabidopsis thaliana*. *npj Systems Biology and Applications*, 5(1), 1–11. https://doi.org/10.1038/s41540-018-0080-1

Leegood, R.C., Lea, P.J., Adcock, M.D. & Häusler, R.E. (1995) The regulation and control of photorespiration. *Journal of Experimental Botany*, 46-(special_issue), 1397–1414. https://doi.org/10.1093/jxb/46.special_issue.1397

Li, J., Weraduwage, S.M., Preiser, A.L., Tietz, S., Weise, S.E., Strand, D.D. et al. (2019) A cytosolic bypass and g6p shunt in plants lacking peroxisomal hydroxypyruvate reductase1. *Plant Physiology*, 180(2), 783–792. https://doi.org/10.1104/pp.19.00256

Liang, Y., Wang, J., Zeng, F., Wang, Q., Zhu, L., Li, H. et al. (2021) Photorespiration regulates carbon-nitrogen metabolism by magnesium chelatase D subunit in rice. *Journal of Agricultural and Food Chemistry*, 69(1), 112–125. https://doi.org/10.1021/acs.jafc.0c05809

Liu, S., Ji, C., Wang, C., Chen, J., Jin, Y., Zou, Z. et al. (2018) Climatic role of terrestrial ecosystem under elevated CO2: a bottom-up greenhouse gases budget. *Ecology Letters*, 21(7), 1108–1118. https://doi.org/10.1111/ele.13078

Long, S.P., Ainsworth, E.A., Rogers, A. & Ort, D.R. (2004) Rising atmospheric carbon dioxide: plants FACE the future. *Annual Review of Plant Biology*, 55, 591–628. https://doi.org/10.1146/annurev.arplant.55.031903.141610

Misra, B.B. & Chen, S. (2015) Advances in understanding CO2 responsive plant metabolomes in the era of climate change. *Metabolomics*, 11(6), 1478–1491. https://doi.org/10.1007/s11306-015-0825-4

Nägele, T., Henkel, S., Hörmiller, I., Sauter, T., Sawodny, O., Ederer, M. et al. (2010) Mathematical modeling of the central carbohydrate metabolism in Arabidopsis reveals a substantial regulatory influence of vacuolar invertase on whole plant carbon metabolism. *Plant Physiology*, 153(1), 260–272. https://doi.org/10.1104/pp.110.154443

Nunes-Nesi, A., Fernie, A.R. & Stitt, M. (2010) Metabolic and signaling aspects underpinning the regulation of plant carbon nitrogen interactions. *Molecular Plant*, 3(6), 973–996. https://doi.org/10.1093/mp/ssq049

Paul, M.J. & Driscoll, S.P. (1997) Sugar repression of photosynthesis: the role of carbohydrates in signalling nitrogen deficiency through source: sink imbalance. *Plant, Cell & Environment*, 20(1), 110–116. https://doi.org/10.1046/j.1365-3040.1997.d01-17.x

Rachmilevitch, S., Cousins, A.B. & Bloom, A.J. (2004) Nitrate assimilation in plant shoots depends on photorespiration. *Proceedings of the National Academy of Sciences of the United States of America*, 101(31), 11506–11510. https://doi.org/10.1073/pnas.0404388101

Renné, P., Dreßen, U., Hebbeker, U., Hille, D., Flügge, U.I., Westhoff, P. et al. (2003) The Arabidopsis mutant dct is deficient in the plastidic glutamate/malate translocator DiT2. *Plant Journal*, 35(3), 316–331. https://doi.org/10.1046/j.1365-313X.2003.01806.x

Sage, R.F. (1994) Acclimation of photosynthesis to increasing atmospheric CO2: the gas exchange perspective. *Photosynthesis Research*, 39(3), 351–368. https://doi.org/10.1007/BF00014591

Seabra, A.R., Silva, L.S. & Carvalho, H.G. (2013) Novel aspects of glutamine synthetase (GS) regulation revealed by a detailed expression analysis of the entire GS gene family of *Medicago truncatula* under different physiological conditions. *BMC Plant Biology*, 13(1), 1–15. https://doi.org/10.1186/1471-2229-13-137

Sengupta, S., Basak, S. & Peters, R.A. (2018) Particle swarm optimization: a survey of historical and recent developments with hybridization perspectives. *ArXiv*, 1–8, 157–191. https://doi.org/10.3390/make1010010

Sharkey, T.D. (1988) Estimating the rate of photorespiration in leaves. *Physiologia Plantarum*, 73(1), 147–152. https://doi.org/10.1111/j.1399-3054.1988.tb09205.x

Shi, S., Xu, X., Dong, X., Xu, C., Qiu, Y. & He, X. (2021) Photosynthetic acclimation and growth responses to elevated CO2 associate with leaf nitrogen and phosphorus concentrations in mulberry (*Morus multicaulis* Perr .). *Forests*, 12(6), 1–14.

Shimono, H., Suzuki, K., Aoki, K., Hasegawa, T. & Okada, M. (2010) Effect of panicle removal on photosynthetic acclimation under elevated CO2 in rice. *Photosynthetica*, 48(4), 530–536. https://doi.org/10.1007/s11099-010-0070-z

Smith, N.G. & Dukes, J.S. (2013) Plant respiration and photosynthesis in global-scale models: incorporating acclimation to temperature and CO2. *Global Change Biology*, 19(1), 45–63. https://doi.org/10.1111/j.1365-2486.2012.02797.x

Solomon, S., Plattner, G.K., Knutti, R. & Friedlingstein, P. (2009) Irreversible climate change due to carbon dioxide emissions. *Proceedings of the National Academy of Sciences of the United States of America*, 106(6), 1704–1709. https://doi.org/10.1073/pnas.0812721106

Sweetlove, L.J., Beard, K.F.M., Nunes-Nesi, A., Fernie, A.R. & Ratcliffe, R.G. (2010) Not just a circle: flux modes in the plant TCA cycle. *Trends in Plant Science*, 15(8), 462–470. https://doi.org/10.1016/j.tplants.2010.05.006

Tcherkez, G., Gauthier, P., Buckley, T.N., Busch, F.A., Barbour, M.M., Bruhn, D., Heskel, M.A., Gong, X.Y. & Crous, K.Y. (2017) Leaf day respiration: low CO2 flux but high significance for metabolism and carbon balance. *New Phytologist*, 216, 986–1001. https://doi.org/10.1111/nph.14816

Tcherkez, G., Mahé, A., Gauthier, P., Mauve, C., Gout, E., Bligny, R., Cornic, G. & Hodges, M. (2009) In Folio Respiratory Fluxomics Revealed by 13C Isotopic Labeling and H/D Isotope Effects Highlight the Noncyclic Nature of the Tricarboxylic Acid "Cycle" in Illuminated Leaves. *Plant Physiology*, 151, 620–630. https://doi.org/10.1104/pp.109.142976

Timm, S., Florian, A., Jahnke, K., Nunes-Nesi, A., Fernie, A.R. & Bauwe, H. (2010) The hydroxypyruvate-reducing system in arabidopsis: multiple enzymes for the same end. *Plant Physiology*, 155(2), 694–705. https://doi.org/10.1104/pp.110.166538

Timm, S., Nunes-Nesi, A., Florian, A., Eisenhut, M., Morgenthal, K., Wirtz, M. et al. (2021) Metabolite profiling in *Arabidopsis thaliana* with moderately impaired photorespiration reveals novel metabolic links and compensatory mechanisms of photorespiration. *Metabolites*, 11(6), 391. https://doi.org/10.3390/metabo11060391

Timm, S., Nunes-Nesi, A., Pärnik, T., Morgenthal, K., Wienkoop, S., Keerberg, O. et al. (2008) A cytosolic pathway for the conversion of hydroxypyruvate to glycerate during photorespiration in Arabidopsis. *Plant Cell*, 20(10), 2848–2859. https://doi.org/10.1105/tpc.108.062265

Wang, F., Gao, J., Yong, J.W.H., Wang, Q., Ma, J. & He, X. (2020) Higher atmospheric CO2 levels favor C3 plants over C4 plants in utilizing ammonium as a nitrogen source. *Frontiers in Plant Science*, 11-(December), 1–16. https://doi.org/10.3389/fpls.2020.537443

Watanabe, C.K., Sato, S., Yanagisawa, S., Uesono, Y., Terashima, I. & Noguchi, K. (2014) Effects of elevated CO2 on levels of primary metabolites and transcripts of genes encoding respiratory enzymes and their diurnal patterns in *Arabidopsis thaliana*: possible relationships with respiratory rates. *Plant and Cell Physiology*, 55(2), 341–357. https://doi.org/10.1093/pcp/pct185

Wong, S.C. (1990) Elevated atmospheric partial pressure of CO2 and plant growth - II. Non-structural carbohydrate content in cotton plants and its effect on growth parameters. *Photosynthesis Research*, 23(2), 171–180. https://doi.org/10.1007/BF00035008

SUPPORTING INFORMATION

Additional supporting information may be found in the online version of the article at the publisher's website.

How to cite this article: Krämer, K., Kepp, G., Brock, J., Stutz, S. & Heyer, A.G. (2022) Acclimation to elevated CO_2 affects the C/N balance by reducing de novo N-assimilation. *Physiologia Plantarum*, 174(1), e13615. Available from: https://doi.org/10.1111/ppl.13615